

Supplementary Information

Salt-induced Fmoc-tripeptide Supramolecular Hydrogels: A Combined Experimental and Computational Study of the Self-assembly

Miryam Criado-Gonzalez,^{a,b*} Mario Iván Peñas,^{a,b} Florent Barbault,^c Alejandro J. Müller,^{b,d}

Fouzia Boulmedais,^e Rebeca Hernández^a

^a Instituto de Ciencia y Tecnología de Polímeros (ICTP-CSIC), 28006 Madrid, Spain

^b POLYMAT and Department of Polymers and Advanced Materials: Physics, Chemistry and Technology, Faculty of Chemistry, University of the Basque Country UPV/EHU, 20018 Donostia-San Sebastián, Spain

^c ITODYS, Université de Paris, CNRS, F75006 Paris, France

^d Ikerbasque, Basque Foundation for Science, Plaza Euskadi 5, 48009 Bilbao, Spain

^e Université de Strasbourg, CNRS, Institut Charles Sadron (UPR 22), 67034 Strasbourg, France

*E-mail: miryam.criado@ehu.es

High-Performance Liquid Chromatography (HPLC) of Fmoc-FFpY

Analytical column type: Phenomenex Luna 3u C18(2) 3 μ m (4.6 \times 150mm \times 3 μ m).

Detector wavelength: 220 nm

Pump A: 0.1% trifluoroacetic in 100% water

Pump B: 0.1% trifluoroacetic in 100% acetonitrile

Elution conditions: 20% ACN+ 80% H₂O

Flow rate: 0.8 mL/min

Injection volume: 30 μ L

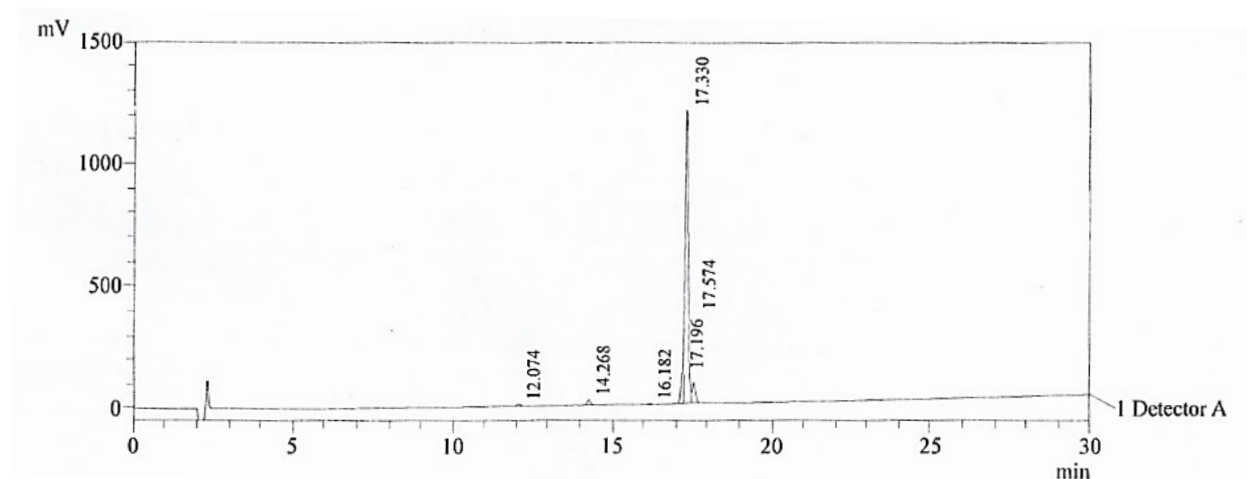


Fig. S1. HPLC spectrum of Fmoc-FFpY.

Table S1. HPLC data of Fmoc-FFpY.

Peak	Retention time (min)	Area	Height	% Area
1	12.074	40621	6136	0.413
2	14.268	154320	22065	1.569
3	16.182	21258	3320	0.216
4	17.196	549682	122487	5.588
5	17.330	8493392	1195352	86.341
6	17.574	577749	81534	5.873
Total		9837022	1430893	100.000

Mass spectrometry of Fmoc-FFpY

Dissolution method: 3% HAC + 25% ACN+ 72% H₂O

Nebulizing Gas Flow: 1.5 mL/min

Detector: -0.2 kv

CDL Temperature: 250 °C

Flow rate: 0.2 mL/min

Injection volume: 1 μL

Block Temperature: 200 °C

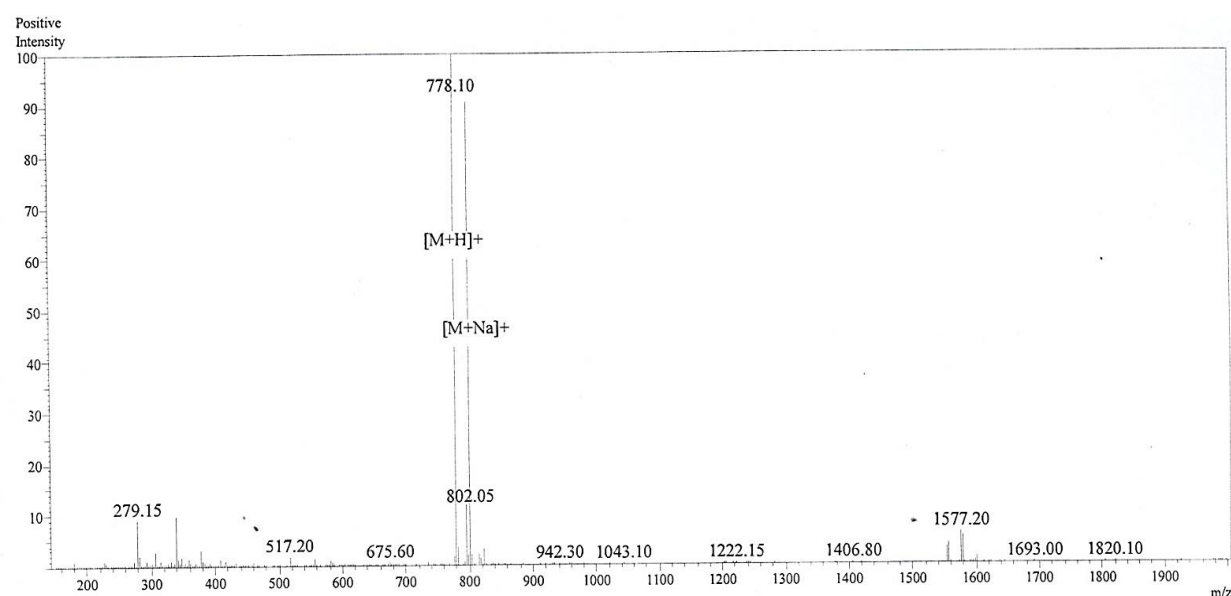


Fig. S2. Mass spectrum of Fmoc-FFpY. The observed molecular weight is 777.10 Da (*the theoretical molecular weight is 777.54 Da).

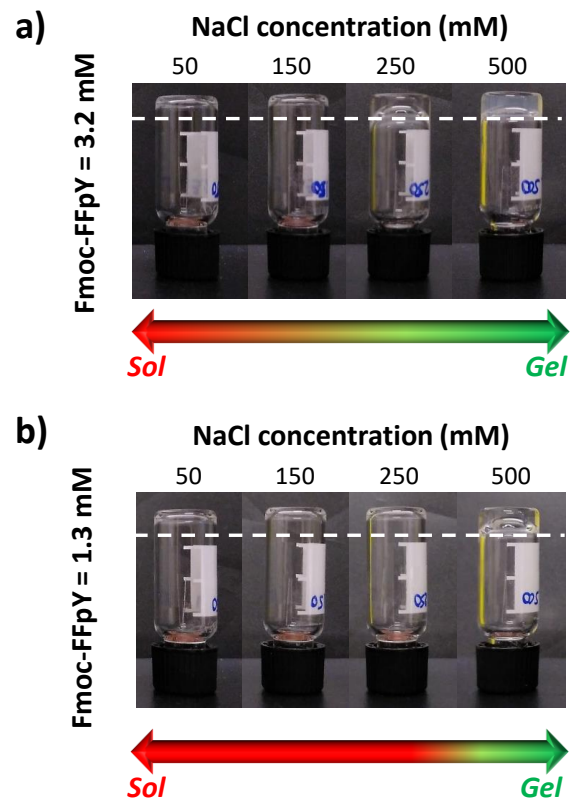


Fig. S3. Inverted tube tests of Fmoc-FFpY/ Na^+ mixtures formed at a fixed concentration of Fmoc-FFpY of (a) 3.2 and (b) 1.3 mM after 24 h. Dashed lines are a guide to the eye.

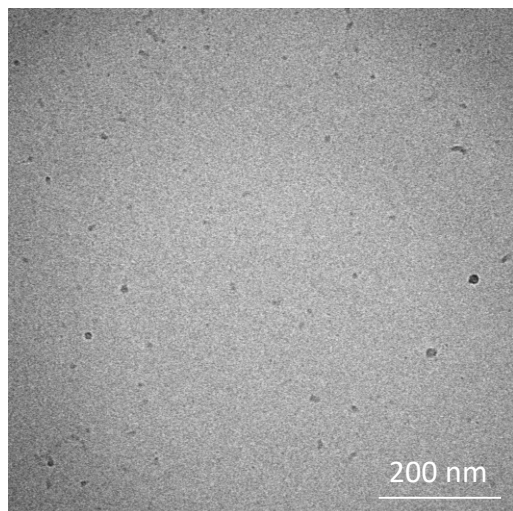


Fig. S4. TEM micrograph of negatively stained Fmoc-FFpY6.4 in solution.

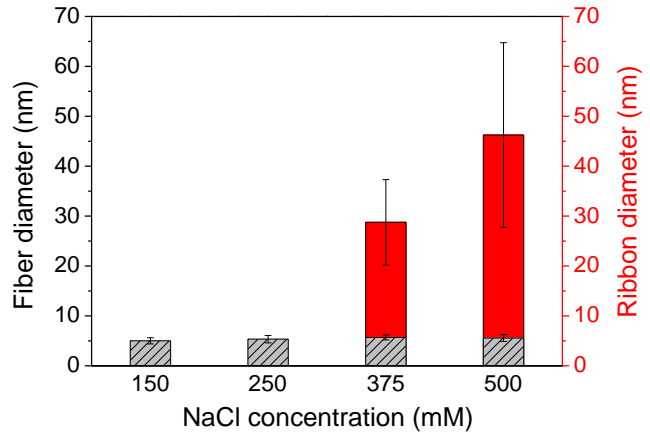


Fig. S5. Fiber (grey bars) and ribbon diameters (red bars) of Fmoc-FFpY6.4/Na⁺ hydrogels prepared in different NaCl concentrations, obtained by measuring the average of 20 fibers or ribbons from TEM micrographs using the software ImageJ.

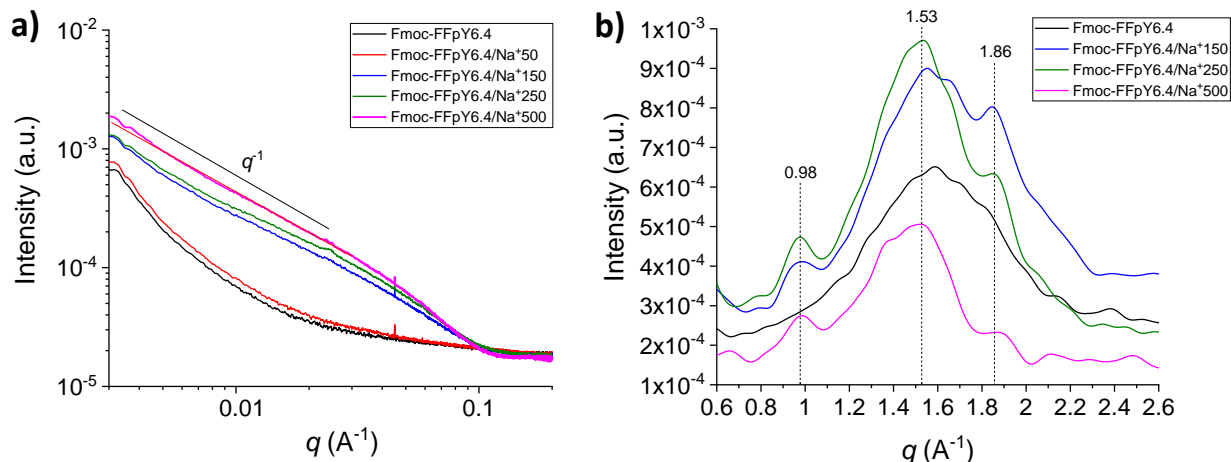


Fig. S6. (a) SAXS scattering curves of Fmoc-FFpY in solution in the absence (black curve) and the presence of different NaCl concentrations: Fmoc-FFpY6.4/Na⁺50 (red curve), Fmoc-FFpY6.4/Na⁺150 (blue curve), Fmoc-FFpY6.4/Na⁺250 (green curve), and Fmoc-FFpY6.4/Na⁺500 (pink curve). For easier visualization, the Fig. displays the q^{-1} relationship at low q angles in SAXS curves. (b) WAXS scattering curves of Fmoc-FFpY in solution in the absence (black curve) and the presence of different NaCl concentrations: Fmoc-FFpY6.4/Na⁺150 (blue curve), Fmoc-FFpY6.4/Na⁺250 (green curve), and Fmoc-FFpY6.4/Na⁺500 (pink curve).

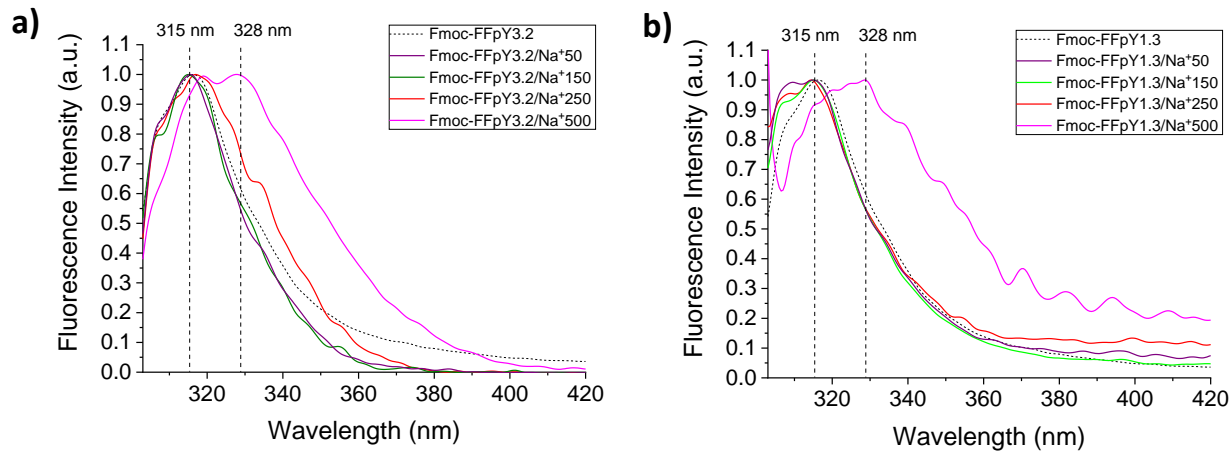


Fig. S7. Fluorescence spectra of different Fmoc-FFpY/Na⁺ mixtures formed at a fixed concentration of Fmoc-FFpY of (a) 3.2 mM and (b) 1.3 mM after 24 h, and in different NaCl concentrations: Fmoc-FFpY/Na⁺50 (purple curve), Fmoc-FFpY/Na⁺150 (green curve), Fmoc-FFpY/Na⁺250 (red curve), and Fmoc-FFpY/Na⁺500 (pink curve).

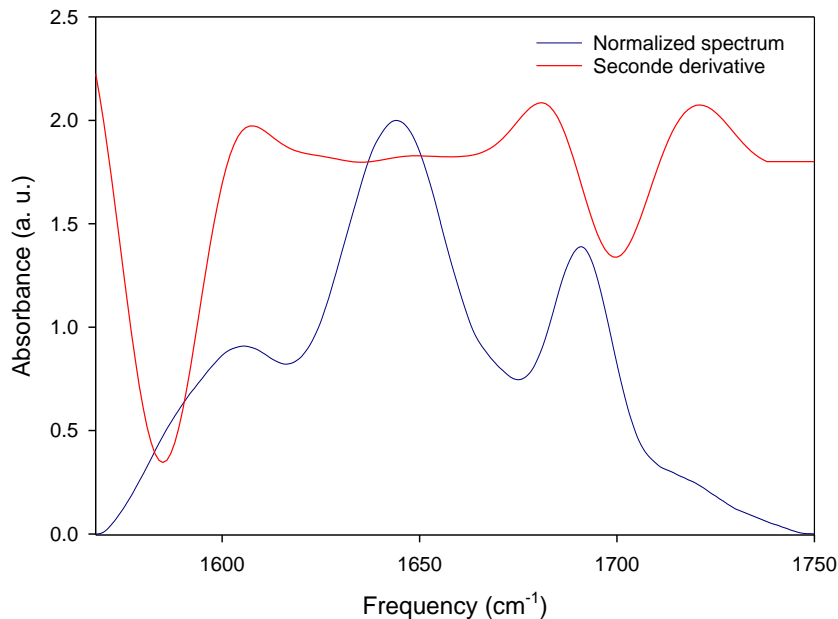


Fig. S8. FTIR normalized spectrum of Fmoc-FFpY6.4/Na⁺500 hydrogel and its second derivative spectra obtained by using OPUS 7.5 software. The minimum position, 1585, 1616, 1635, 1661, and 1698 cm⁻¹, were used for the decomposition of the region.

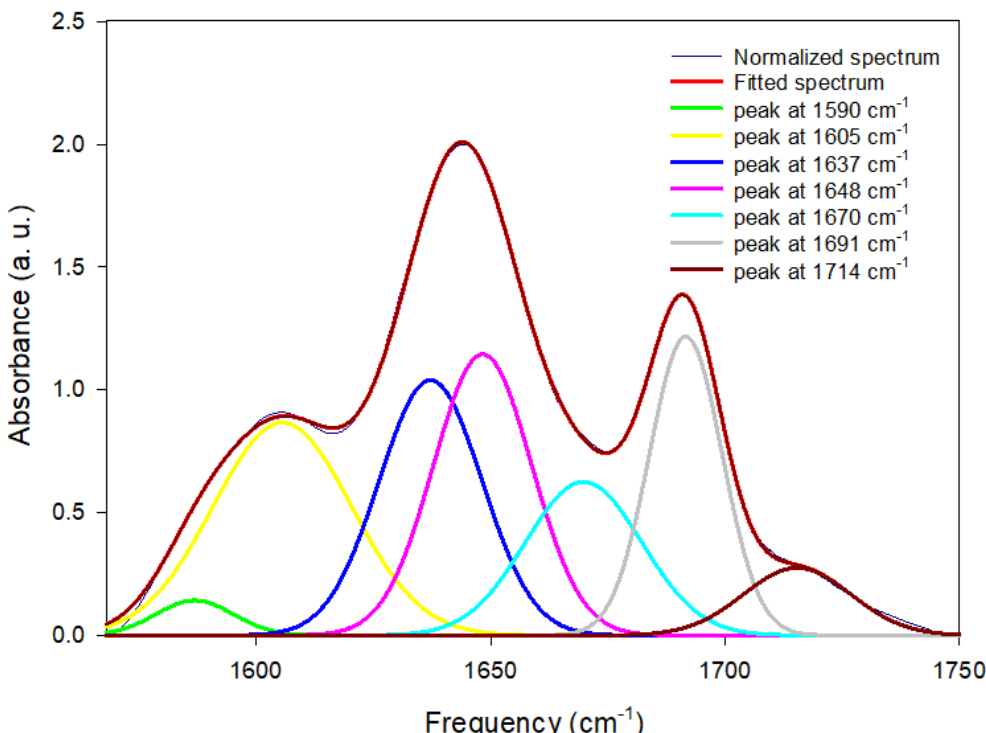


Fig. S9. FTIR normalized spectrum of the amide I band region of Fmoc-FFpY6.4/ Na^+ 500 hydrogel. This region was fitted by multiple Gaussian peaks using OPUS 7.5 software.

Table S2. The relative content of the different secondary structure contributions of the amide I band of Fmoc-FFpY6.4/ Na^+ 500 hydrogel. The peaks were attributed according to Xing et al. *Angew. Chem. Int. Ed* 2018, 57, 1537 and T. H Kim et al. *Arch. Pharm. Res.* 2007, 30, 381.

Structure	Peaks (cm^{-1})	Contribution in the amide I band (%)
C=O of COO ^a	1591	-
β -sheet	1610	21
Random	1637	30
α -helix	1649	29
Antiparallel β -sheet	1670	20
Carbamate	1692	-
C=O carbonyl involved in H bonds	1714	-

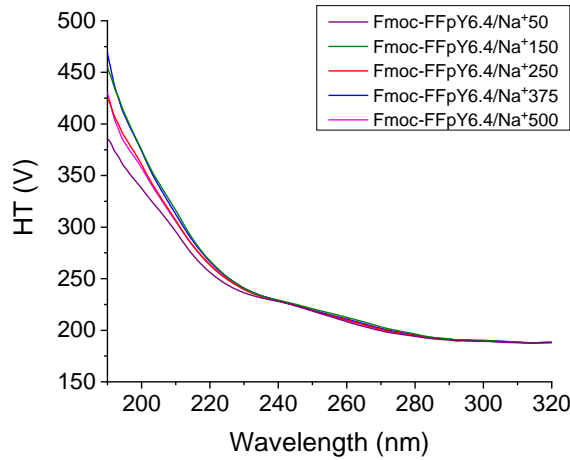


Fig. S10. Voltage curves of CD measurements of Fmoc-FFpY/Na⁺ mixtures: Fmoc6.4/Na⁺50, Fmoc6.4/Na⁺150, Fmoc6.4/Na⁺250, Fmoc6.4/Na⁺375, and Fmoc6.4/Na⁺500.

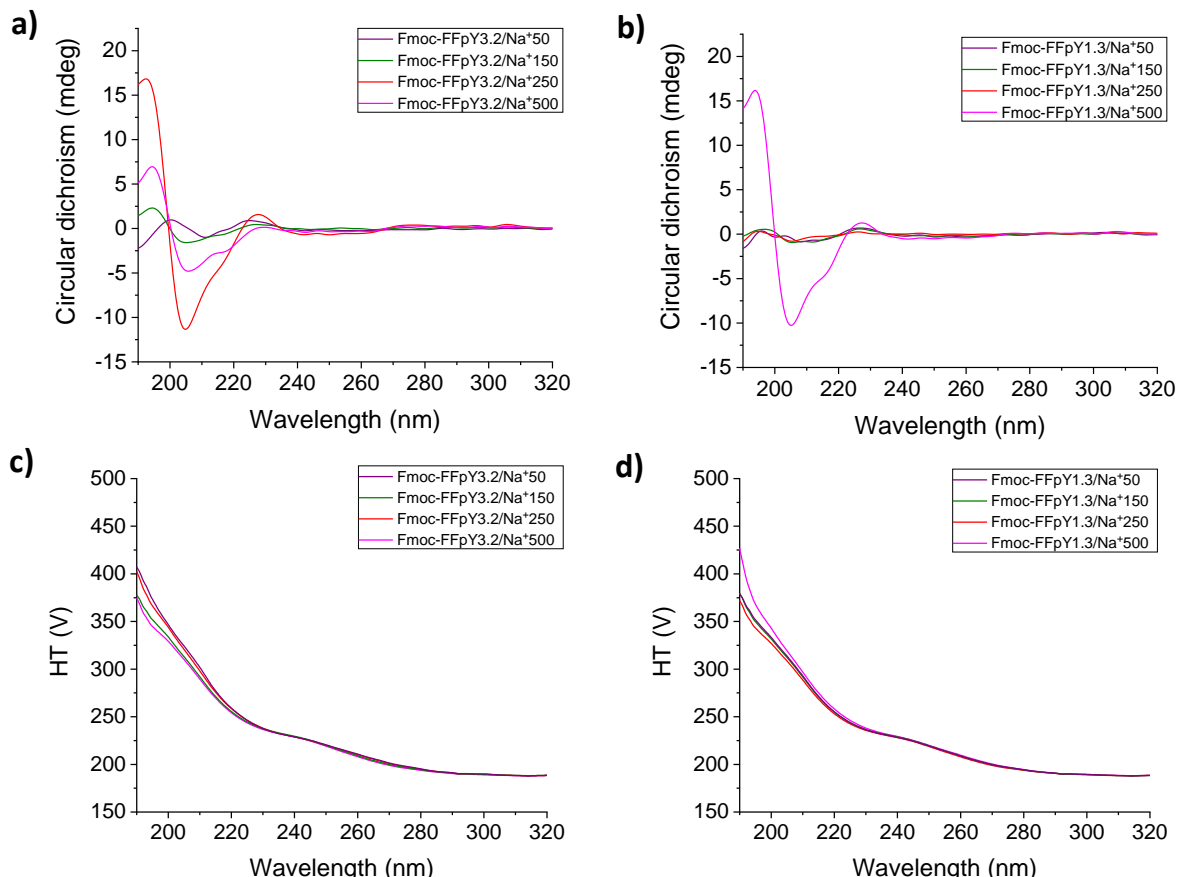


Fig. S11. (a, b) CD spectra and (c, d) voltage curves of Fmoc-FFpY/Na⁺ mixtures formed at a fixed concentration of Fmoc-FFpY of (a, c) 3.2 and (b, d) 1.3 mM after 24 h, and different NaCl concentrations: Fmoc-FFpY/Na⁺50 (purple curve), Fmoc-FFpY/Na⁺150 (green curve), Fmoc-FFpY/Na⁺250 (red curve), Fmoc-FFpY/Na⁺375 (blue curve), and Fmoc-FFpY/Na⁺500 (pink curve).

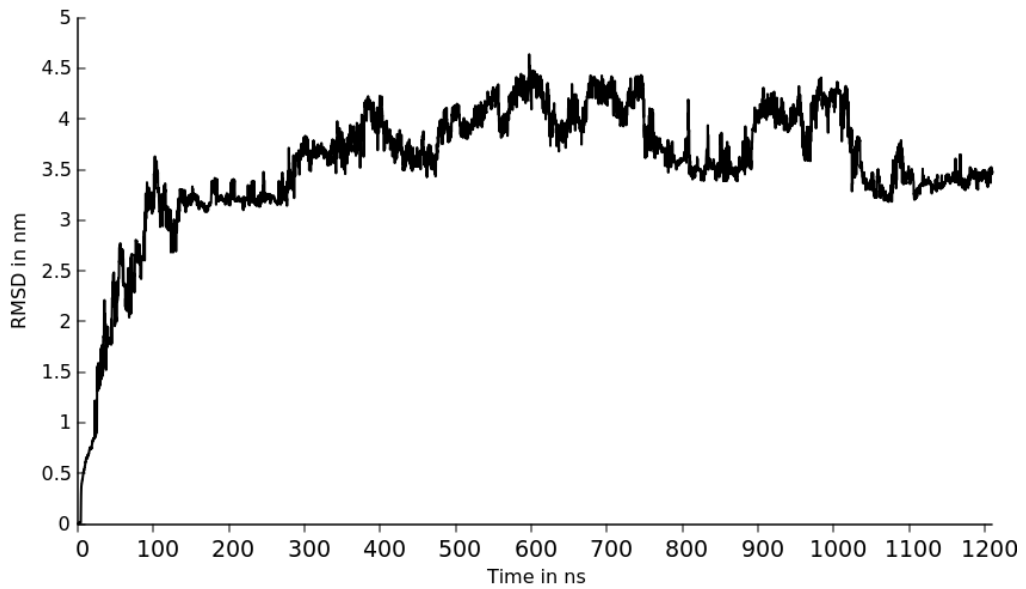


Fig. S12. Example of RMSD curves for a MD simulation investigating the structural assembly of 40 Fmoc-FFpY peptide units.

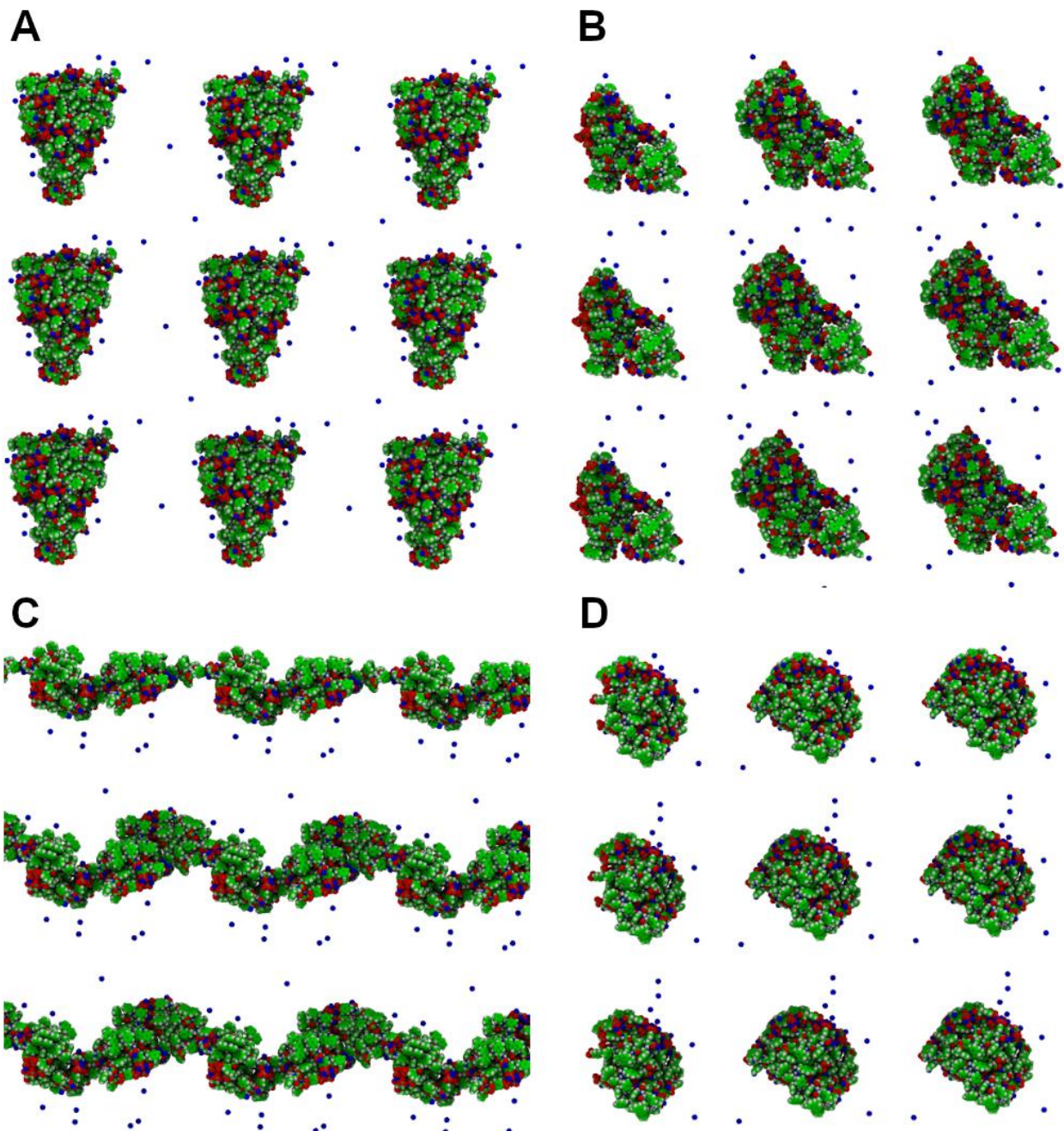


Fig. S13. Final structures obtained for the four replicas of MD simulations at 250 mM of NaCl. 3 of the studied system collapsed while one, C, take advantage of the periodic conditions to generate a ribbon-like structuration.

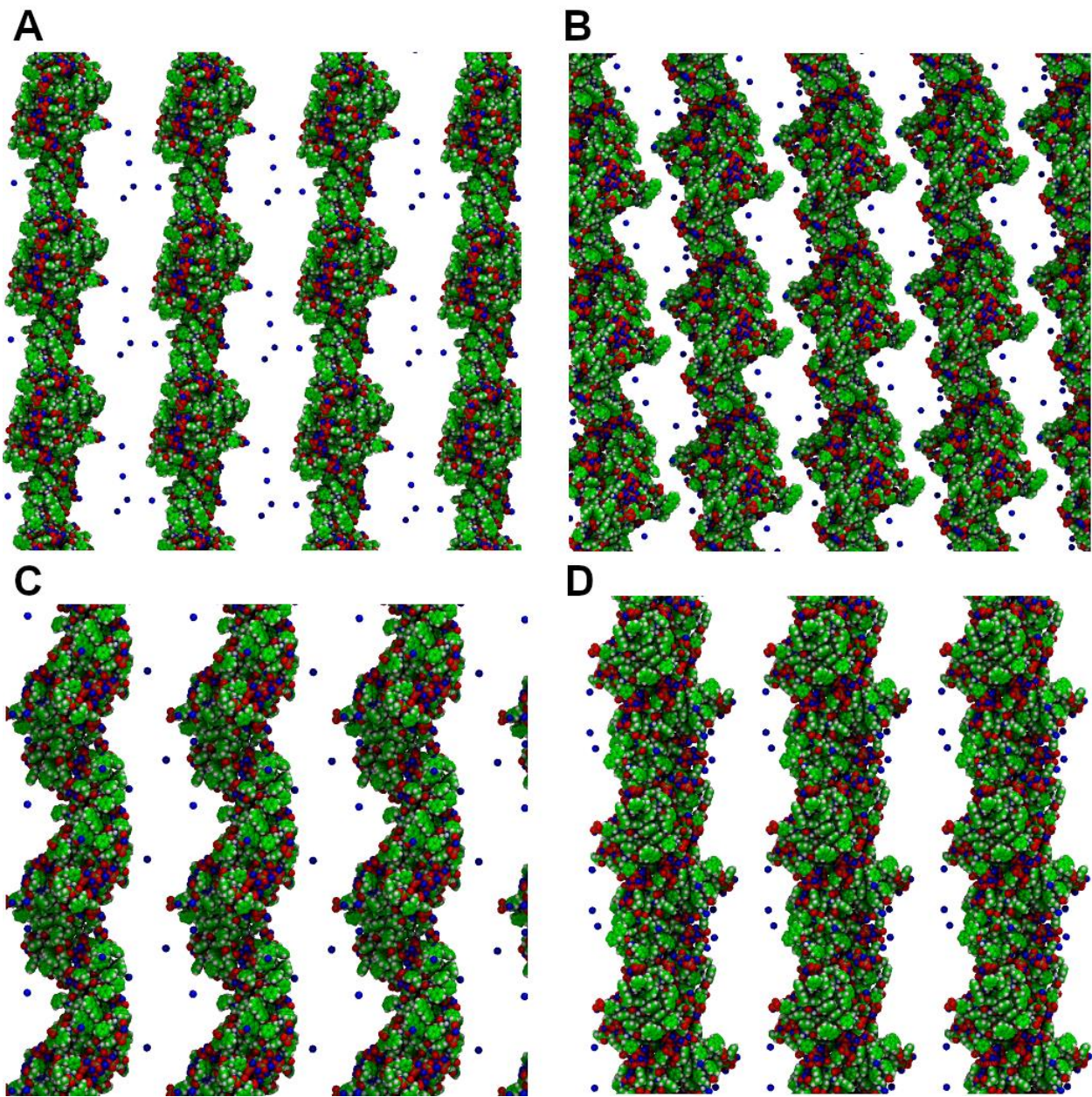


Fig. S14. Final structures obtained for the four replicas of MD simulations at 500 mM of NaCl. For each simulated system, a ribbon-like structure is observed.

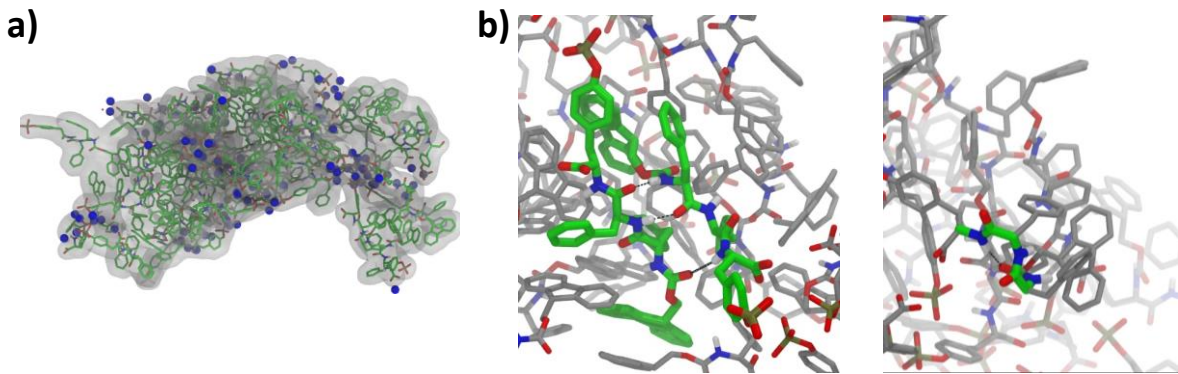


Fig. S15. Molecular Dynamics simulation where 40 Fmoc-FFpY units are assembled in presence of 500 mM NaCl. (a) Representation of the localization of Na^+ ions (blue spheres) in the vicinity of the 40 Fmoc-FFpY units assembled. (b) β -sheet structure involving 3 hydrogen bonds (left) and α -helix structure involving one intramolecular hydrogen bond (right). In the right Fig. only the peptide structure is shown in green color to distinguish the helicoidal organization.

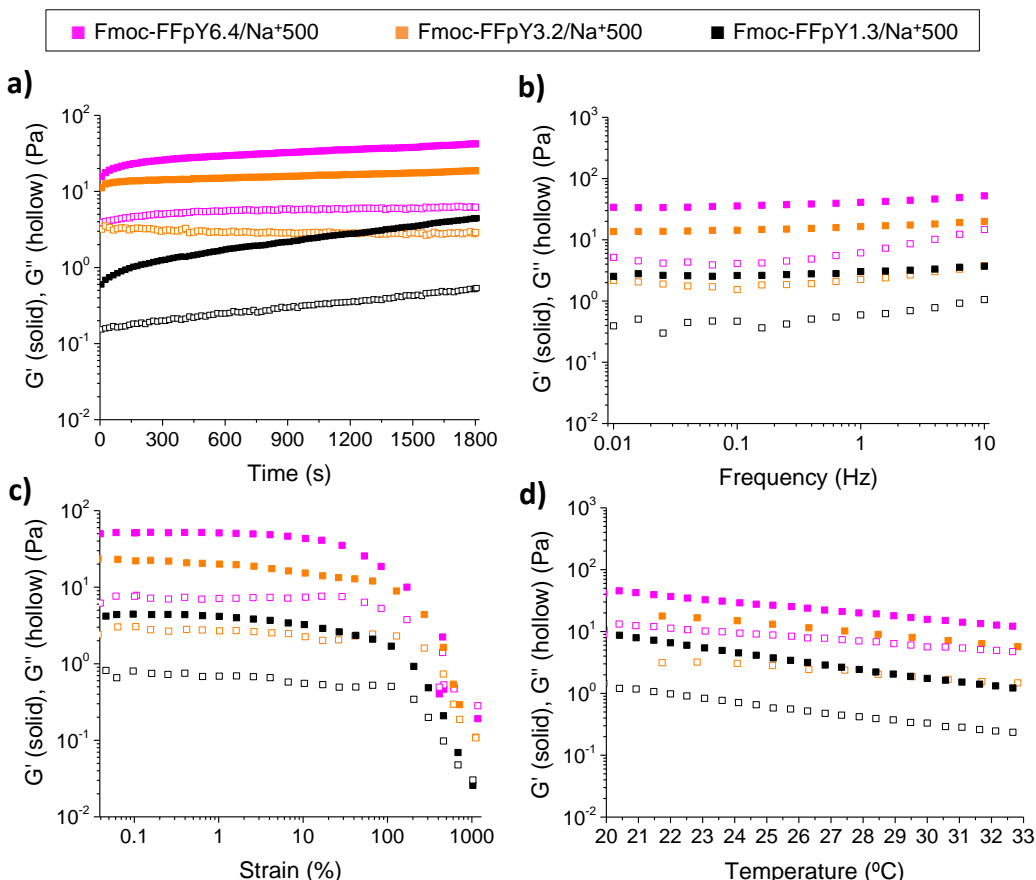


Fig. S16. Rheological properties of Fmoc-FFpY/Na⁺500 hydrogels prepared at 1.3 (■), 3.2 mM (□), and 6.4 mM (■) Fmoc-FFpY. Storage modulus (G' - solid symbols) and loss modulus (G'' - hollow symbols) as a function of the (a) time (1 Hz, 1% strain), (b) frequency (0.01–10 Hz, 1% strain), and (c) strain (0.01–1000%, 1 Hz) at 20 °C, and (d) temperature (1% or 1000% strain).

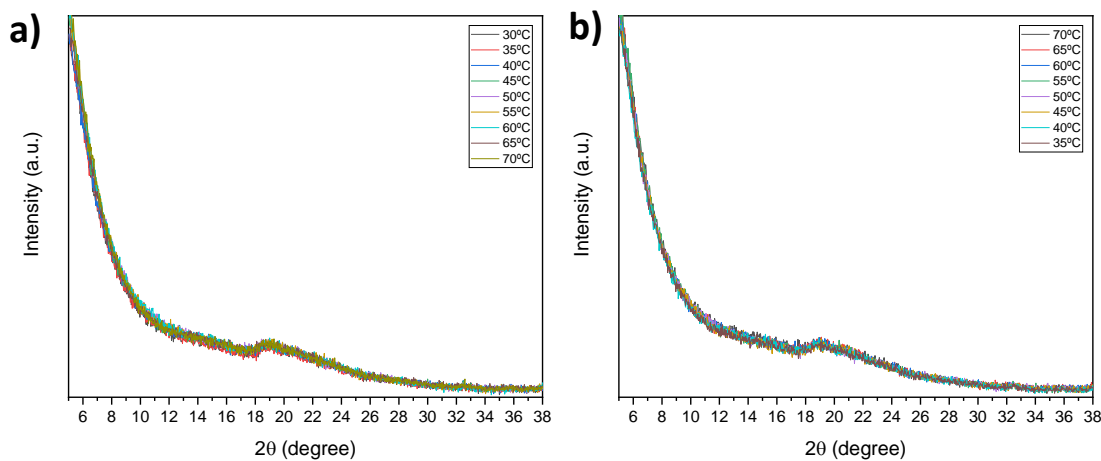


Fig. S17. X-ray diffractograms of Fmoc-FFpY in powder during (a) the heating process and (b) the subsequent cooling. X-ray diffractograms of Fmoc-FFpY in the powder were recorded with a Philips X'Pert PRO with Cu K α radiation in the Bragg-Brentano geometry in the range of $2\theta = 5$ -38°. Measurements were first performed during heating from 30 °C up to 70 °C at a heating rate of 5 °C min-1, and then during cooling from 70 °C up to 35 °C at a cooling rate of 5 °C min-1.

Table S3. Heating and cooling enthalpies and transition temperatures obtained through micro DSC measurements.

Sample	1 st Heating		1 st Cooling		2 nd Heating		2 nd Cooling	
	T _{g-s} (°C)	ΔH _{g-s} (J g ⁻¹)	T _{s-g} (°C)	ΔH _{s-g} (J g ⁻¹)	T _{g-s} (°C)	ΔH _{g-s} (J g ⁻¹)	T _{s-g} (°C)	ΔH _{s-g} (J g ⁻¹)
Fmoc-FFpY6.4	62	16.0	47	19.7	62	15.8	46	19.7
Fmoc-FFpY6.4/Na ⁺ 150	62	11.3	47	14.8	62	10.7	47	15.0
Fmoc-FFpY6.4/Na ⁺ 250	62	5.9	48	8.0	62	6.7	48	8.6
Fmoc-FFpY6.4/Na ⁺ 375	53	5.8	40	10.2	54	3.8	44	10.0
Fmoc-FFpY6.4/Na ⁺ 500	62	35.4	45	39.1	62	34.4	46	39.5